Ultrafast Optical Spin Echo for Electron Spins in Semiconductors

Susan M. Clark,[1,*] Kai-Mei C. Fu,[2] Qiang Zhang,[1,3] Thaddeus D. Ladd,[1,3] Colin Stanley,[4] and Yoshihisa Yamamoto[1,3]

[1]*Edward L. Ginzton Laboratory, Stanford University, Stanford, California 94305-4088, USA*

[2]*Information and Quantum Systems, Hewlett-Packard Laboratories, 1501 Page Mill Road, MS1123, Palo Alto, California 94304, USA*

[3]*National Institute of Informatics, 2-1-2 Hitotsubashi, Chiyoda-ku, Tokyo 101-8430, Japan*

[4]*Department of Electronics and Electrical Engineering, Oakfield Avenue, University of Glasgow, Glasgow, G12 8LT, United Kingdom*

(Received 3 April 2009; published 19 June 2009)

Spin-based quantum computing and magnetic resonance techniques rely on the ability to measure the coherence time T_2 of a spin system. We report on the experimental implementation of all-optical spin echo to determine the T_2 time of a semiconductor electron-spin system. We use three ultrafast optical pulses to rotate spins an arbitrary angle and measure an echo signal as the time between pulses is lengthened. Unlike previous spin-echo techniques using microwaves, ultrafast optical pulses allow clean T_2 measurements of systems with dephasing times (T_2^*) fast in comparison to the time scale for microwave control. This demonstration provides a step toward ultrafast optical dynamic decoupling of spin-based qubits.

DOI: 10.1103/PhysRevLett.102.247601 PACS numbers: 76.60.Lz, 03.67.Lx, 32.80.Qk, 33.35.+r

Proposals for spin-based quantum information processors have generated renewed interest in the coherent control and decoherence of electron spins in many environments. Determining the decoherence time T_2 for semiconductor spins is particularly important since it sets the time scale for error correction in a semiconductor-spin-based quantum computer [1–3]. Also, the measurement of T_2 provides information about noise processes in a spin's environment and is the basis for many techniques in magnetic resonance spectroscopy and magnetic resonance imaging.

In some systems, however, inhomogeneous spin environments obscure a measurement of T_2. Spin inhomogeneity causes a perceived loss of coherence, or static dephasing, on a faster time scale called T_2^*. For a spin ensemble, this inhomogeneity is due to local environments causing spins to have different Larmor frequencies [4,5]. For a single spin, this inhomogeneity is caused by slow environmental changes during temporal averaging [6–8]. Techniques exist to decouple spins from these inhomogeneities [9], but they rely on the coherent control of the spin. If T_2^* is fast compared to the spin manipulation time, these techniques become ineffective. One solution is to use a faster method of spin control. Here, we use ultrafast optical pulses [5,10–14] to control the spins instead of slower microwave pulses. Ultrafast optical pulses not only allow efficient refocusing of static dephasing caused by inhomogeneities, but may also provide sufficient speed to enable dynamic decoupling of spins from the noise sources that cause T_2 decoherence [15–19].

The simplest method to measure T_2 is the Hahn spin-echo sequence [20], which consists of a $\pi/2$ pulse, a period of free evolution, a π pulse, and then another equal period of free evolution. This sequence is a workhorse technique in the fields of nuclear magnetic resonance (NMR) and electron-spin resonance (ESR). Recently, this technique has been used to measure T_2 for potential solid-state spin qubits [6–8,21,22]. Another, more indirect, way to measure T_2 is via pulsed mode locking. For this method, trains of ultrafast optical pulses are applied to a system and a T_2 may be extracted by comparing the amount of generated coherence for different pulse train repetition times [23]. Mode locking, however, preserves only a particular coherence determined by the polarization of the rotation pulses, unlike spin-echo techniques which preserve any state of a qubit, including entangled states used in quantum computing. This mode-locking technique has recently been modified to observe optical spin-echo signals [24], but no measurement of T_2 has been made with these echo signals.

The Hahn spin-echo technique may be generalized to arbitrary spin-rotation angles. A spin rotation of angle θ due to an ultrafast pulse is modeled as an instantaneous, effective field along the x axis much larger than the applied magnetic field in the z direction. As a result, the rotation is described by an instantaneous unitary rotation operator $R_x(\theta) = \exp(-i\theta S^x)$ for the Pauli spin-operator S^x ($S = 1/2$). Similarly, free rotation about the magnetic field is modeled by a unitary rotation operator about the z axis, $R_z(\phi)$. The angle of rotation is determined by $\phi = \omega_n \tau$, where τ is the time of free procession and $\omega_n = g\mu_B B^z(\mathbf{r}_n)/\hbar$ is the Larmor frequency of the nth spin. Here, g is the gyromagnetic ratio for the material, μ_B is the Bohr magneton, and $B^z(\mathbf{r}_n)$ is the magnetic field at each spin position $\mathbf{r}_n$. The Larmor frequency varies among spins primarily due to random nuclear hyperfine fields. Assuming we begin with the nth spin initialized in the down state $|\downarrow\rangle$ after a sequence of three ultrafast rotations of angles θ_1, θ_2, and θ_3, separated by two intervals of free precession, τ_1 and τ_2, the final state of the system, $|\psi_f\rangle_n$, can be described by

$$|\psi_f\rangle_n = R_x(\theta_3)R_z(\omega_n\tau_2)R_x(\theta_2)R_z(\omega_n\tau_1)R_x(\theta_1)|\downarrow\rangle. \quad (1)$$

In our experiment, we measure probability P that a spin flips to the up state, $|\uparrow\rangle$, averaged over N spins. To model inhomogeneity, we let the Larmor frequencies have a

Gaussian probability distribution, and the average projection becomes

$$P = \frac{1}{N}\sum_{n=1}^{N} |\langle\uparrow|\psi_f\rangle_n|^2 = \frac{1}{\sqrt{2\pi}\sigma}\int_{-\infty}^{\infty} d\omega |a(\omega)|^2 e^{-(\omega-\omega_0)^2/2\sigma^2}, \tag{2}$$

where ω_0 is the mean of the spin resonance distribution, $\sigma \sim 1/T_2^*$ is the width of the distribution, and $a(\omega)$ is the probability amplitude of a spin with Larmor frequency ω to be in the up state. The average projection on the z axis is then found to be

$$\begin{aligned}\langle\sigma^z(\tau_1,\tau_2)\rangle &= 2P-1 \\ &= -\cos\theta_3\cos\theta_2\cos\theta_1 + \cos\theta_3\sin\theta_2\sin\theta_1\cos(\omega_0\tau_1)e^{-(1/2)\sigma^2\tau_1^2} + \sin\theta_3\sin\theta_2\cos\theta_1\cos(\omega_0\tau_2)e^{-(1/2)\sigma^2\tau_2^2} \\ &\quad + \sin\theta_3\cos^2\frac{\theta_2}{2}\sin\theta_1\cos[\omega_0(\tau_1+\tau_2)]e^{-(1/2)\sigma^2(\tau_1+\tau_2)^2} - \sin\theta_3\sin^2\frac{\theta_2}{2}\sin\theta_1\cos[\omega_0(\tau_1-\tau_2)]e^{-(1/2)\sigma^2(\tau_1-\tau_2)^2}.\end{aligned} \tag{3}$$

Most of the terms in Eq. (3) result in polarizations that rapidly vanish due to T_2^* dephasing, but the last term describes a spin echo which is immune to this dephasing. This term is maximized for the Hahn echo condition $\theta_1 = \theta_3 = \pi/2$ and $\theta_2 = \pi$. The Hahn echo condition, however, is not required for an echo; there will be a finite polarization for almost any angle of the three pulses (Fig. 1 panels). This generalization is important for ultrafast pulses, because pulse-induced decoherence may increase with angle [12].

We applied this sequence of three optical rotations to an ensemble of electron spins bound to neutral Si donors in GaAs at low temperature (1.5 K) [25]. The ground states are denoted $|0\rangle$ and $|1\rangle$ depending on the spin projection of the electron, m_e, and are split by an energy $\hbar\omega_L \approx 50$ GHz via a magnetic field, $B_{\text{ext}} = 10$ T [Fig. 2(a)]. In Voigt geometry, these ground states are optically connected to the donor-bound-exciton (D^0X) states, $|e\rangle$, which consist of an additional electron-hole pair forming an electron-spin singlet ($m_s = 0$), and a hole spin with projection m_h. Despite the many D^0X states, we can approximate the ground states as a two-level system via adiabatic elimination of the excited states (valid if the detuning, $\Delta = 1$ THz, is much larger than other rates in the system). The ultrafast pulse (2 ps) couples states $|0\rangle$ and $|1\rangle$ with an effective Rabi frequency $\Omega_e \sim \Omega^2/\Delta$, where Ω is the instantaneous optical Rabi frequency of the pulse before adiabatic elimination [3,12,14]. For our experiments, the pulse width is constant, so the pulse power determines the spin-rotation angle. In this material, high pulse powers induce additional decoherence, limiting θ to values less than about $\pi/3$ [12]. For efficient rotations, we experimentally determined the

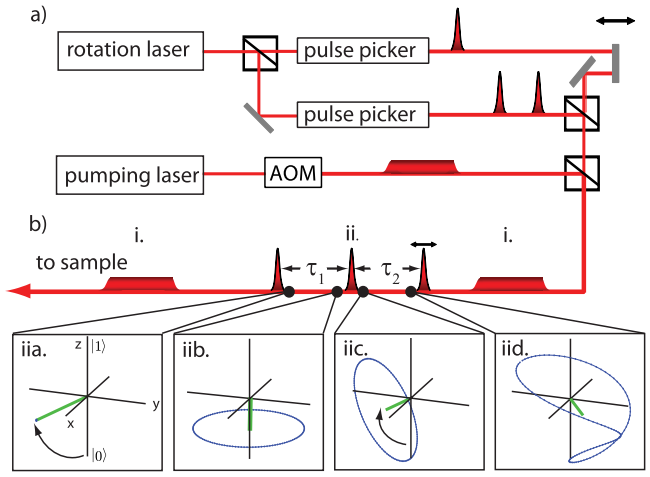

FIG. 1 (color online). (a) Experimental setup to generate optical pulse sequence. (b) The pulse sequence: labels i and ii match those in Fig. 2(b). Panels show an inhomogenous spin ensemble (blue dots) on the Bloch sphere at different times during a $\pi/3 - \pi/3 - \pi/3$ pulse sequence. The green or gray line shows the average spin polarization vector. After the final ultrafast pulse and pumping pulse, the average spin polarization vector shown in panel iid will be proportional to the spin polarization that we observe on the z axis.

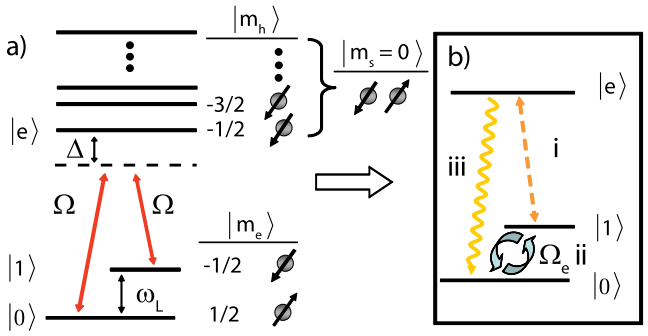

FIG. 2 (color online). (a) Energy level diagram of donor-bound-exciton system in a magnetic field: ground states $|0\rangle$ and $|1\rangle$ are split by an energy $\hbar\omega_L$. They are optically connected to the donor-bound-exciton states, $|e\rangle$, via an ultrafast pulse of Rabi frequency Ω detuned by Δ. (b) Relevant energy levels and applied optical fields: the pumping laser applies electric fields on resonance to pump population to the $|0\rangle$ state (orange dashed line, i). The rotation laser performs rotations between the ground states with effective Rabi frequency Ω_e (blue arrows, ii). The pumping laser applies another field on resonance (i) and light is collected from the $|0\rangle \leftrightarrow |e\rangle$ transition (yellow line, iii).

optimum optical polarization of the applied pulse to be linearly polarized 45° from the magnetic field axis [12].

The experimental setup to generate this pulse sequence is shown in Fig. 1(a) and the pulse sequence used to perform the spin-echo measurement is depicted in Fig. 1(b). First we initialize the spins to the $|0\rangle$ state by applying a long pulse (μs) from a continuous-wave ring laser (''pumping laser'') gated by an acousto-optic modulator (AOM) resonant on the $|1\rangle \leftrightarrow |e\rangle$ transition [labeled i in Figs. 1(b) and 2(b)]. The first and second rotation pulses are picked from the pulse train of a Ti:sapphire mode-locked laser (''rotation laser'') by a pulse picker [electro-optic modulator (EOM) followed by an AOM for improved extinction ratio] and are separated by τ_1, which is always a multiple of the repetition time of the laser (13 ns). The third pulse arrives at a time τ_2 after the second pulse, which is determined by both a pulse picker and an optical delay line which can vary τ_2 by tens of picoseconds. In order to measure rephasing, the difference between the free evolution times, $|\tau_2 - \tau_1|$, is kept smaller than the 1 ns T_2^* dephasing time [4]. We determine the final state of the system by projecting the rephased spin polarization vector onto the z axis with the application of another long pulse from the pumping laser on resonance with the $|1\rangle \leftrightarrow |e\rangle$ transition. We monitor the spontaneous emission at the frequency of the $|0\rangle \leftrightarrow |e\rangle$ transition [labeled iii in Fig. 2(b)], which will be proportional to the amount of population in state $|1\rangle$. We measure this signal with an avalanche photodiode after filtering out pump laser scatter via a monochromator and polarization selection rules.

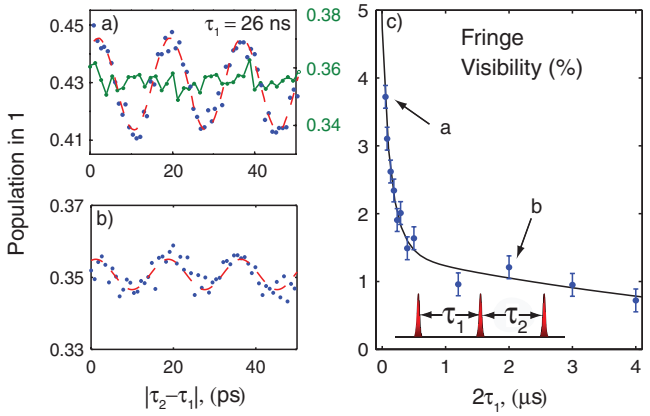

FIG. 3 (color online). Results of all-optical spin-echo experiment. (a) Population in $|1\rangle$ (green solid line) as a second pulse is scanned in a two pulse experiment with $\tau_1 = 26$ ns. No fringes can be seen, indicating complete dephasing. Population in $|1\rangle$ (blue dots) and a fit (red dashed line) to a three pulse experiment with $\tau_1 = 26$ ns. Here, there are clear oscillations. (b) Data and fit to a three pulse experiment with $2\tau_1 = 2$ μs. Visibility has decreased compared to (a). (c) Fringe visibility vs pulse separation, $2\tau_1$. Error bars are calculated from the standard deviation of several measurements of the fringe visibility at one point. The fit (black line) is a phenomenological decay that includes pulse-induced decoherence and intrinsic T_2 decoherence with a decay time of 6.7 ± 2.5 μs. The points shown in (a) and (b) are labeled.

For these ultrafast rotations, only the arrival time of the pulse determines the phase of the rotation [3], so the optical phase of the pulse does not need to be externally stabilized. However, the uncertainty of the pulse arrival time needs to be much less than the Larmor period of the spin system. The jitter of the mode-locked laser was measured using a technique described by von der Linde [26] and was found to be about 1 ps over a millisecond time scale. By keeping τ_1 and τ_2 less than a millisecond, individual pulses picked from the mode-locked train can be used for this pulse sequence without external stabilization.

The results of the experiment can be seen in Fig. 3. When we apply only two pulses, as in a Ramsey fringe experiment, we see no fringes [Fig. 3(a), solid green line] for pulse separations greater than 26 ns, indicating that the spins are completely dephased. When we add a third pulse, we recover fringes that have a frequency equal to the Larmor frequency [blue dots and red dashed line in Figs. 3(a) and 3(b)] which is evidence of the echo. Some fluctuations in the experiment cause a small linear drift of random direction and amplitude in the overall detector count rate. We remove the drift by fitting each fringe curve to a sum of terms constant, linear, and oscillatory in τ_2, and then subtracting the linear term. We calculate the visibility for each fringe curve as $V = (\max - \min)/(\max + \min)$, where max and min are the maximum and minimum amplitudes of the fitted sine curve. In Fig. 3(c) we see the decay of the fringe visibility with pulse separation, indicating decoherence in this system.

The data in Fig. 3(c) are well described by a phenomenological model with two sources of decoherence. The first source is intrinsic to the sample and leads to a decay of the echo with rate T_2^{-1}. The second source is generated by the pulses themselves. It was found in Ref. [12] that there is additional dephasing of the bound-exciton state proportional to applied pulse power. This dephasing may be due to local heating via background absorption of the laser, which induces some population of phonons or other excitations, such as excited impurity states. In our model, these pulse-induced remnant excitations decohere the spins at a rate proportional to their population. Since the spurious excitation is assumed to equilibrate at some time scale T_h, we presume this effect causes an induced decoherence time R^{-1} that vanishes as $\exp(-t/T_h)$. A coherence $\langle \sigma^+ \rangle$ then obeys a Bloch equation of the form

$$\frac{d}{dt}\langle \sigma^+(t)\rangle_n = \left[i\omega_n - \frac{1}{T_2} - Re^{-t/T_h} \right] \langle \sigma^+(t)\rangle_n, \qquad (4)$$

which may be analytically integrated.

Using this decoherence model, the visibility for $\tau_1 = \tau_2 = \tau \gg T_2^* \sim 1/\sigma$ is

$$V(\tau) = V_0 e^{-2\tau/T_2 - 2RT_h[1-\exp(-\tau/T_h)]}. \qquad (5)$$

This curve is fit to the visibility data in Fig. 3(c) (black line). The resulting fitting parameters are the intrinsic decoherence time $T_2 = 6.7 \pm 2.5$ μs, the pulse-induced decoherence time $R^{-1} = 175 \pm 30$ ns, the relaxation rate of the excitations contributing to pulse-induced decoherence $T_h = 100 \pm 20$ ns, and the initial visibility before decay $V_0 = 0.047 \pm 0.003$. This last parameter V_0 may be estimated from Eq. (3) as

$$V_0 = \langle \sigma^z \rangle_0 \frac{D(\theta_1) D(\theta_2) \sin(\theta_3) \sin(\theta_2^2/2) \sin(\theta_1)}{1 - \langle \sigma^z \rangle_0 \cos(\theta_3) \cos(\theta_2) \cos(\theta_1)}, \quad (6)$$

where $\langle \sigma^z \rangle_0$ is the initial polarization created by optical pumping and $D(\theta)$ is the spin decoherence created by a single pulse of angle θ. Both of these may be estimated from previous studies [12] as $D(\theta) \approx 1 - 0.25\theta$ and $\langle \sigma^z \rangle \approx 0.9$, leading to a V_0 of 5%, in agreement with the fit.

The measured $T_2 = 6.7 \pm 2.5$ μs is consistent with previous measures of T_2 in quantum dot systems using microwave spin echo [6,7] and mode locking [23]. This time scale is shorter than the lifetime-limited maximum $2T_1$ [27], which has been measured to be milliseconds in this sample [28]. Some form of dynamic decoherence limits T_2; the likely source is nuclear spin diffusion, which has been theoretically predicted to cause coherence decay on this time scale [29–31]. This and other types of dynamic decoherence, however, can be reversed using a series of π pulses applied faster than the characteristic time scale of decoherence [15–19], extending the T_2 time of the system. When π pulses are not possible, several small-angle pulses can be applied over multiple Larmor periods to sum to a π pulse [12]. Because optical pulses can be applied more quickly than microwave pulses, the demonstration in this Letter is a critical step toward eliminating fast decoherence, potentially making many more materials suitable for applications requiring long T_2.

In conclusion, we demonstrated that three ultrafast optical pulses can produce an echo signal to measure the T_2 time of electron-spin systems. Although here we apply this technique to Si:GaAs, we believe it has potential applications in other materials relevant to magnetic resonance, particularly those with fast decoherence times. We have also demonstrated that partial rephasing is possible even when π and $\pi/2$ pulses are unavailable, meaning the technique can be applied when a system has a small optical dipole moment, when only low laser power is available, or when optical dephasing is present. Last, optical pulses have the potential to extend the decoherence time in semiconductor systems by dynamical decoupling. Such a scheme could be used to extend the spin-memory time of a spin-based quantum computer and can be integrated into quantum bus schemes for quantum computing [3].

S. M. C. was partially supported by HP through the Center for Integrated Systems. This work was financially supported by the MURI Center for photonic quantum information systems (ARO/ARDA Program DAAD 19-03-1-0199), JST/SORST program for the research of quantum information systems for which light is used, University of Tokyo Special Coordination Funds for Promoting Science and Technology, NIST (70NANB6H6163), and MEXT, NICT.

*sclark4@stanford.edu

[1] D. Loss and D. P. DiVincenzo, Phys. Rev. A **57**, 120 (1998).
[2] A. Imamoglu *et al.*, Phys. Rev. Lett. **83**, 4204 (1999).
[3] S. M. Clark, K.-M. C. Fu, T. D. Ladd, and Y. Yamamoto, Phys. Rev. Lett. **99**, 040501 (2007).
[4] K.-M. C. Fu *et al.*, Phys. Rev. Lett. **95**, 187405 (2005).
[5] M. V. G. Dutt *et al.*, Phys. Rev. B **74**, 125306 (2006).
[6] J. R. Petta *et al.*, Science **309**, 2180 (2005).
[7] F. H. L. Koppens, K. C. Nowack, and L. M. K. Vandersypen, Phys. Rev. Lett. **100**, 236802 (2008).
[8] R. Hanson, V. V. Dobrovitski, A. E. Feiguin, O. Gywat, and D. D. Awschalom, Science **320**, 352 (2008).
[9] C. P. Slichter, *Principles of Magnetic Resonance* (Springer, New York, 1996).
[10] J. A. Gupta, R. Knobel, N. Samarth, and D. D. Awschalom, Science **292**, 2458 (2001).
[11] S. E. Economou, L. J. Sham, Y. Wu, and D. G. Steel, Phys. Rev. B **74**, 205415 (2006).
[12] K.-M. C. Fu, S. M. Clark, C. Santori, C. Stanley, M. C. Holland, and Y. Yamamoto, Nature Phys. **4**, 780 (2008).
[13] J. Berezovsky, M. H. Mikkelsen, N. G. Stoltz, L. A. Coldren, and D. D. Awschalom, Science **320**, 349 (2008).
[14] D. Press, T. D. Ladd, B. Zhang, and Y. Yamamoto, Nature (London) **456**, 218 (2008).
[15] L. Viola and S. Lloyd, Phys. Rev. A **58**, 2733 (1998).
[16] W. M. Witzel and S. Das Sarma, Phys. Rev. Lett. **98**, 077601 (2007).
[17] W. Yao, R.-B. Liu, and L. J. Sham, Phys. Rev. Lett. **98**, 077602 (2007).
[18] G. S. Uhrig, Phys. Rev. Lett. **98**, 100504 (2007).
[19] B. Lee, W. M. Witzel, and S. Das Sarma, Phys. Rev. Lett. **100**, 160505 (2008).
[20] E. L. Hahn, Phys. Rev. **80**, 580 (1950).
[21] F. Jelezko, T. Gaebel, I. Popa, A. Gruber, and J. Wrachtrup, Phys. Rev. Lett. **92**, 076401 (2004).
[22] R. Hanson, O. Gywat, and D. D. Awschalom, Phys. Rev. B **74**, 161203(R) (2006).
[23] A. Greilich *et al.*, Science **313**, 341 (2006).
[24] A. Greilich *et al.*, Nature Phys. **5**, 262 (2009).
[25] V. A. Karasyuk *et al.*, Phys. Rev. B **49**, 16 381 (1994).
[26] D. von der Linde, Appl. Phys. B **39**, 201 (1986).
[27] W. A. Coish and D. Loss, Phys. Rev. B **70**, 195340 (2004).
[28] K.-M. C. Fu, W. Yeo, S. Clark, C. Santori, C. Stanley, M. C. Holland, and Y. Yamamoto, Phys. Rev. B **74**, 121304(R) (2006).
[29] D. Paget, Phys. Rev. B **25**, 4444 (1982).
[30] R. de Sousa and S. Das Sarma, Phys. Rev. B **67**, 033301 (2003).
[31] W. Yao, R.-B. Liu, and L. J. Sham, Phys. Rev. B **74**, 195301 (2006).